Published in final edited form as:
J Vis. ; 10(11): 4. doi:10.1167/10.11.4.

Combination of rod and cone inputs in parasol ganglion cells of the magnocellular pathway

Dingcai Cao,
Sections of Surgical Research and Ophthalmology and Visual Science, Department of Surgery, University of Chicago, Chicago, IL, USA

Barry B. Lee, and
SUNY College of Optometry, New York, NY, USA, & Max Planck Institute for Biological Chemistry, Göttingen, Germany

Hao Sun
Department of Optometry and Visual Sciences, Buskerud University College, Kongsberg, Norway

Dingcai Cao: d-cao@uchicago.edu; Barry B. Lee: blee@sunyopt.edu; Hao Sun: hao.sun@hibu.no

Abstract

This study investigates how rod and cone inputs are combined in the magnocellular (MC) pathway in the mesopic luminance range, when both rods and cones are active. Responses of parafoveal MC ganglion cells from macaque retina were measured as a function of temporal frequency (0.62–20 Hz) or contrast (0.05–0.55) at mesopic light levels (0.2, 2, 20, and 200 td). Stimuli were of three modulation types: (1) isolated rod stimuli (only rod signals were modulated), (2) isolated cone stimuli (only cone luminance signals from long- and middle-wavelength sensitive cones were modulated), and (3) combined rod and cone stimuli (both rod and cone luminance signals were modulated in phase, as with conventional stimuli). The results showed that under mesopic conditions, the relative rod and cone inputs to the MC cells varied with light level and they are combined linearly prior to saturation. Further, rod contrast gain is relatively stable over the mesopic range while cone contrast gain increased with light level. Finally, the measured rod and cone inputs are consistent with the measured human temporal contrast sensitivity functions under comparable stimulation conditions.

Keywords

contrast gain; electrophysiology; ganglion cells; photoreceptors; rod vision; contrast sensitivity

Introduction

Compared with cone-mediated photopic vision or rod-mediated scotopic vision, mesopic vision is more complex because it involves both rods and cones, i.e., rod and cone signals interact with each other to contribute to our vision. Psychophysically, the activation of rods at mesopic light levels alters many cone-dependent visual functions and perceptions (reviewed by Buck, 2004), including color appearance (Buck, Knight, & Bechtold, 2000; Cao, Pokorny, & Smith, 2005; Cao, Pokorny, Smith, & Zele, 2008), chromatic discrimination (Cao, Zele, &

Corresponding author: Dingcai Cao., d-cao@uchicago.edu., Address: 5841.S. Maryland Ave., MC2114 Chicago, Illinois, USA.
Commercial relationships: none.

Pokorny, 2008; Stabell & Stabell, 1977), and temporal processing (Cao, Zele, & Pokorny, 2006, 2007; Zele, Cao, & Pokorny, 2008).

Modern anatomical and physiological studies have identified three major neural retinogeniculate pathways in the primate visual system that convey retinal information to visual cortex, the magnocellular (MC), parvocellular (PC), and koniocellular (KC) pathways (reviewed by Dacey, 2000). The pathways are named after different layers of lateral geniculate nucleus (LGN) that receive inputs from distinct types of retinal ganglion cells and project to different areas of primary visual cortex. These parallel pathways have distinctive temporal, spatial, chromatic, and contrast response characteristics and are thought to mediate different aspects of vision (Lee, Martin, & Valberg, 1989): the MC pathway underlies a psychophysical luminance channel, while PC and KC pathways underlie channels associated with red–green and blue–yellow chromatic visions (Pokorny & Smith, 2004).

Anatomical and single-unit electrophysiological studies have shown that rods and cones share certain neural pathways and have joint inputs to retinal ganglion cells (reviewed by Daw, Jensen, & Brunken, 1990; Sharpe & Stockman, 1999). Rod signals are thought to be conveyed by two primary pathways: one pathway via ON rod bipolars, AII amacrine cells, and ON and OFF cone bipolars; and the other via rod–cone gap junctions and ON and OFF cone bipolars. The role of these two pathways is thought to vary with illumination level. The first rod pathway is a high-gain pathway and is hypothesized to mediate rod vision at low light levels, while the second pathway is relatively low gain and is hypothesized to mediate rod vision at high scotopic and mesopic light levels.

Several primate physiological studies have identified rod inputs to the MC pathway (Gouras & Link, 1966; Lee, Smith, Pokorny, & Kremers, 1997; Virsu & Lee, 1983; Virsu, Lee, & Creutzfeldt, 1987), the PC pathway (Lee et al., 1997; Virsu et al., 1987; Wiesel & Hubel, 1966), and the KC pathway (Crook et al., 2009; Field et al., 2009; Virsu & Lee, 1983; Virsu et al., 1987). Identification of rod inputs is the first step; a further question is how rod and cone signals are combined to contribute to visual function. The challenge for assessing the combination of rod and cone signals is to generate separate stimuli that activate rods alone, or cones alone, at the same chromaticity and adaptation level. With a four-primary photostimulator (Pokorny, Smithson, & Quinlan, 2004), it is possible to provide such stimuli and measure ganglion cell responses in different pathways to isolated rod or cone stimuli.

In this study, we focused on rod and cone inputs to the parasol ganglion cells in the MC pathway, because strong rod and cone inputs to the MC ganglion cells have been found at mesopic light levels (Lee et al., 1997) and these should allow for reliable assessment of the combination of rod and cone inputs at these light levels. We measured ganglion cell responses to rod modulation alone, cone modulation alone, and combined rod and cone modulation, at a number of temporal frequencies, contrasts, and retinal illuminance levels. The MC cell responses were correlated with human temporal contrast sensitivity functions measured with comparable stimuli.

Methods

Animal preparation

Macaques (*M. fascicularis* or *M. radiata*) were sedated with an intramuscular injection of ketamine (10 mg/kg). Anesthesia was continued with 10 mg/kg thiopental and further maintained with isoflurane (0.2%–2%) in a 70%:30% nitrous oxide and oxygen mixture. Electroencephalogram (EEG), electrocardiogram (ECG), heart rate, temperature, and end-tidal CO_2 level were monitored continuously to ensure adequate depth of anesthesia. Muscle relaxation was maintained by continuous infusion of gallamine triethiodide (5 mg/kg per hour,

intravenously) with accompanying dextrose Ringer's solution (6 ml/kg/h). The body temperature was kept close to 37.5°C by an electric heating pad. End-tidal CO_2 was brought close to 4% by adjusting the rate of respiration. All procedures were approved by the SUNY Animal Care Committee and conform to Association for Research in Vision and Ophthalmology guidelines for ethical care of animals.

Cell classification and recording

Neuronal activity was recorded from retinal ganglion cells by tungsten-in-glass electrodes inserted through a cannula entering the eye behind the limbus (Crook, Lange-Malecki, Lee, & Valberg, 1988). Cell classification (MC, PC, or KC) was based on cell responses to achromatic and chromatic stimuli (Lee et al., 1989). MC cells were generally identified by their phasic responses, lack of spectral opponency, and high responsivity to achromatic contrast. Additional tests, e.g., measuring responses to heterochromatically modulated lights (Smith, Lee, Pokorny, Martin, & Valberg, 1992) was employed in cases when classification was difficult. The majority of MC cells we recorded ($N = 14$) were between 3° and 15° eccentricities. We also deliberately sampled 5 MC cells at an eccentricity higher than 20° to investigate the association between cell responses and eccentricity.

Apparatus and calibration

We used two identical four-primary photostimulators, one at the State University of New York College of Optometry for physiological measurements and another set at the University of Chicago for psychophysical measurements. Both were designed and constructed at the University of Chicago. The four-primary photostimulators consist of two channels; one provides a center field and the other a surround field. Each channel has 4 LEDs that can be modulated separately. The four primary wavelengths for both the center and surround stimuli are 460 nm, 516 nm, 558 nm, and 660 nm, all with half-bandwidths of about 10 nm. Using the method of silent substitution (Estévez & Spekreijse, 1982), the four primary lights of each channel can allow independent stimulation of the rods and the L, M, and S cones (details see Shapiro, Pokorny, & Smith, 1996). Independent control of rod and cone excitations can be understood in terms of color matching. For instance, in color matching, the chromaticity of an equal-energy spectrum light can be matched by a combination of three primaries (460, 516, and 660 nm). The same chromaticity can be matched by another set of primaries (460, 558, and 660 nm). When the two sets of primaries match in chromaticity, they produce the same L-, M-, and S-cone excitations. Note that the two sets of primaries differ in one primary, with the rods being more sensitive to the 516-nm light than to the 558-nm light. Varying the proportion of the two matches over time produces rod modulation while maintaining constant cone excitations. A similar approach can be applied to isolate L-, M-, and S-cone excitations. The full technical and design aspects of the photostimulator are given by Pokorny et al. (2004; Pokorny & Cao, 2010) and examples of its implementation can be found in Cao, et al. (2005), Sun, Pokorny, & Smith (2001a; 2001b), and Zele, et al. (2007; 2008).

For physiological measurements, the radiances of the primaries were controlled by National Instruments (Austin, TX) interface boards hosted in a Macintosh Quadra 950 computer. For psychophysical measurements, the radiances of the primaries were controlled by an eight-channel analog output Dolby sound card (M-Audio-Revolution 7.1 PCI) hosted in a Macintosh G5 PowerPC computer. The output of the sound card was demodulated (Puts, Pokorny, Quinlan, & Glennie, 2005), and the slow amplitude modulation of the sound-card signal was then used to modulate the LED output via a voltage-to-frequency converter (Swanson, Ueno, Smith, & Pokorny, 1987).

The four-primary photostimulators were calibrated to provide precise rod and cone stimulations. The calibration included the measurement of the spectral and luminance outputs

of each LED and the linearization of the light output of each LED as a function of input voltage. The psychophysical measurements also included an observer calibration procedure that corrected for individual differences in prereceptoral filtering. Details of the calibration procedure are described elsewhere (Cao et al., 2005).

Stimuli

Comparable stimuli were used for both physiological and psychophysical measurements. Isolated rod modulation (Rod), or isolated cone luminance modulation (L + M + S), or combined rod and cone modulation (L + M + S + Rod) was generated by the four-primary photostimulators. Changes in mean luminance was achieved with neutral density filters, while the modulation in photo-receptor excitations remained the same. Since S-cones and rods do not contribute to cone-defined luminance, changes in S-cone and rod stimulations alter chromaticity and rod excitation only. Note that, in a cone-based chromaticity space, luminance is typically specified as (L + M) (Smith & Pokorny, 1996). Here, we used (L + M + S) for cone luminance stimulus specification because, to maintain equal chromaticity while modulating luminance, S-cone excitation has to be varied in the same proportion as L- and M-cone excitations. We normalized rod excitations such that for an equal-energy-spectrum light, 1 photopic Troland (td) light had 1 rod td (Shapiro et al., 1996).

For physiological measurements, full-field circular stimuli (4.7° in diameter) were used. The time-averaged chromaticity of the light was set to L/(L + M) = 0.75, S/(L + M) = 0.25 to achieve a large range of contrast for rod or cone modulation. The rod and/or cone excitations were modulated sinusoidally. For measurements of temporal frequency response functions of all of the stimulus types (isolated rod modulation, isolated cone modulation, or combined rod and cone modulation), temporal frequency was varied between 0.61 Hz and 20 Hz while Michelson contrast was fixed at 55%. For measurements of contrast response functions, Michelson contrast was varied between 5% and 55%, while the temporal frequency was fixed at 4.88 Hz. The retinal illuminance was 0.2, 2, 20, or 200 td.

For measurements of human psychophysical temporal contrast sensitivity functions (TCSF), the stimuli were presented as a 4°-diameter circular field with a 10°-diameter surround. The stimulus center was positioned at 6° eccentricity in temporal retina. The rod and/or cone stimulation of the center field were modulated sinusoidally within a 1-s raised cosine envelope to minimize adaptation to the periodically modulated stimuli (Cao et al., 2006). For each stimulus type (isolated rod stimuli, isolated cone stimuli, or combined rod and cone stimuli), the time-averaged chromaticity of the light in the center and surround fields was metameric to the equal-energy-spectrum light [L/(L + M) = 0.667, S/(L + M) = 1.0]. The modulation temporal frequencies ranged between 1 and 32 Hz. The retinal illuminance was 0.2, 2, 20, or 200 td.

Procedure

MC ganglion cell temporal frequency response and contrast response functions were measured from 200 td to 0.2 td, with successive reductions in retinal illuminance level in 1 log unit steps using neutral density filters. At least 4 min of adaptation to each new light level was allowed.

Human TCSFs to the isolated rod stimuli, isolated cone stimuli, and combined rod and cone stimuli were determined by a random dual 2–Yes–1–No staircase procedure, which adjusted modulation contrast depending on the observer's response whether flicker was detected. Each condition was repeated in four sessions for each observer. Two female observers (*AB*, age 21 years; *YL*: age 22 years) with normal vision participated in the study. Observers were dark adapted for 30 min before measurements. All experimental procedures were approved by the Institutional Review Board at the University of Chicago.

Results

MC cell responses as a function of temporal frequency

We recorded responses from 19 MC cells (9 on-center and 10 off-center cells) at each light level. Two cells were not recorded at 0.2 td (both on-center cells) because their responses at 2 td were already very weak. On- and off-center cells had similar response patterns with modulation frequency and retinal illuminance level, except for their response phase difference. Therefore, the response amplitudes of the on- and off-center cells were averaged. Figure 1A shows the average of MC cell 1st harmonic response amplitudes (impulse per second) as a function of temporal frequency, for a modulation contrast of 55%. At 0.2 and 2 td, the MC cell response pattern for the combined rod and cone stimuli (blue triangles) was very similar to that for the isolated rod stimuli (red circles); at 200 td, however, the response pattern for the combined stimuli was comparable to that for the isolated cone stimuli (green squares). At 20 td, the MC cells responded equally well to the isolated rod or cone stimuli. As retinal illuminance increased, the MC cell response amplitude to the isolated rod stimuli increased from 0.2 to 2 td, then decreased at 20 and 200 td. The shape of the temporal response was relatively stable from 0.2 to 20 td although the response peak shifted from 2.44 Hz at 0.2 td to 4.88 Hz at 2 td and 20 td, and to 9.76 Hz at 200 td. For the isolated cone stimuli or the combined stimuli, the overall MC cell response amplitude increased monotonically with increasing light level; the temporal frequency of the response peak also increased markedly with light level.

To assess the strength of rod input relative to cone input, the ratios of response amplitudes between the isolated rod and cone stimuli at each frequency and light level for each cell was computed and the ratios from all of the cells (over all eccentricities) were averaged (Figure 2A, the averaged ratios at 0.2 td are not shown because of weak responses to the isolated cone stimuli). The rod/cone amplitude ratios varied with temporal frequency and light level: at 2 td, the ratios decreased with increasing temporal frequency from 5.5 (≤1.22 Hz) to 3.5 (2.44–9.76 Hz) at 20 and 200 td; however, the ratios remained relatively stable with temporal frequency up to 9.76 Hz, (about 1.5 at 20 td and 0.5 at 200 td), and then decreased at higher frequencies.

Rod input strength might be expected to be correlated with eccentricity due to the increase in the ratio of rod to cone photoreceptor density. The estimated rod/cone ratios at 20 td (when rods and cones had comparable responses) were highly correlated with eccentricity, with higher rod input strength at higher eccentricity (Pearson correlation $r = 0.50–0.78$ at different temporal frequencies, all p-values < 0.05). Figure 2B shows the averaged rod/cone ratios for eccentricities less than 10° (6 cells, mean eccentricity of 5.6°), between 10° and 15° (8 cells, mean eccentricity of 12.4°), and more than 20° (5 cells, mean eccentricity of 25°) at 4.88 Hz and 20 td. The expected rod/cone photoreceptor density ratios at these mean eccentricities should be about 3.5, 15.0, and 66, respectively based on Curcio, Sloan, Kalina, and Hendrickson (1990). The rod/cone response amplitude ratio increases nearly linearly with the photoreceptor density ratio (Pearson correlation $r = 0.98$).

We used the response phases with the isolated rod and cone stimuli to assess the latency difference between rod and cone responses. Figure 3 shows the averaged response phases of selected cells that had good responses to both rod stimuli and cone stimuli (peak response amplitude ≥10 impulses/s at any light level). At intermediate temporal frequencies (between 1 and 10 Hz), the response phases were nearly linearly related to temporal frequencies, suggesting a constant time delay between the rod and cone inputs (Kremers & Scholl, 2001). Therefore, we fitted linear regression lines between phases and temporal frequencies. The differences in slopes between the rod and cone responses were used to estimate the time delays between the rod and cone inputs. Figure 4 shows the distribution of estimated latency difference between rod and cone inputs. The mean rod–cone delay decreased slightly with light level

(33.3 ms at 0.2 td, 30.9 ms at 2 td, 28.2 ms at 20 td, and 27.3 ms at 200 td), but this did not reach significance ($p = 0.11$). The rod–cone delays increased with eccentricity (data not shown).

MC cell responses as a function of contrast

The averaged response amplitudes as a function of modulation contrast at 4.88 Hz for all cells are shown in Figure 1B. The response amplitudes were either linearly related to contrast (all stimulus types at 0.2 td and the isolated rod stimuli at 2 td) or showed some response saturation at high contrasts. The cell response at contrast C, $R(C)$, is described by the Michaelis–Menten saturation function (Kaplan & Shapley, 1986):

$$R(C)=R_0+\frac{R_{\max}C}{C+C_{\text{sat}}}, \tag{1}$$

where R_0 is a baseline term (representing noise in the absence of stimulation), $R_{\max}$ is the maximum response, and C_{sat} is the semi-saturation contrast. When C is much smaller than C_{sat}, Equation 1 approximates a linear function. The contrast gain, g, can be obtained as the first derivative of Equation 1 at zero contrast (Shapley & Enroth-Cugell, 1984), that is

$$g=R_{\max}/C_{\text{sat}}. \tag{2}$$

Typically, in the absence of stimulation, a 1st harmonic amplitude of 0–4 impulses/s was present. Therefore, we set R_0 at 2 impulses/s (Lee, Pokorny, Smith, Martin, & Valberg, 1990). For each cell, we fitted contrast responses with Equation 1 for each stimulus type and at each light level to estimate contrast gain. The averaged contrast gain for each stimulus type is shown in Figure 5. For comparison, MC cell contrast gain estimations from Purpura, Kaplan, and Shapley (1988) are also included (these authors used sinusoidal gratings of 0.6–1.6 cpd drifting at 4.22 Hz). With the combined rod–cone stimuli, the contrast gain at different light levels was closely similar to the averaged contrast gain from Purpura et al.'s values, as shown by the gray dashed line (slope of 0.30 in the log–log plot). The contrast gain with the isolated cone stimuli had the same slope but was about 0.44 log unit lower than those with the combined stimuli. Finally, the contrast gain with isolated rod stimuli increased from 0.2 to 2 td, then remained relatively stable from 2 td to 200 td. The estimated contrast gain with the different stimulus types did not vary with eccentricity (data not shown).

The combination of rod and cone inputs

To evaluate how rod and cone inputs were combined in MC cell responses, we first considered a vector sum model to predict MC cell responses to the combined stimuli based on the responses to the isolated rod and cone stimuli (response-based vector sum model). If MC cell responses (MC_{r} or MC_{c}) to the isolated rod or cone stimuli with a temporal frequency of f are described by a sinusoid with a rod or cone response phase ϕ_{r} or ϕ_{c}:

$$MC_{\text{r}}=A_{\text{r}}\sin(2\pi ft+\phi_{\text{r}}), \tag{3}$$

$$MC_{\text{c}}=A_{\text{c}}\sin(2\pi ft+\phi_{\text{c}}), \tag{4}$$

then predicted MC cell responses to the combined stimuli based on a linear sum of the responses to the isolated rod and cone stimuli are given as

$$MC_{r+c}=A_r\sin(2\pi ft+\phi_r)+A_c\sin(2\pi ft+\phi_c). \quad (5)$$

This model assumes that the rod and cone responses are combined linearly at the ganglion cell level. The predicted MC cell response amplitude (A_{r+c}) and phase (ϕ_{r+c}) are given as

$$A_{r+c}=\sqrt{(A_r^2+A_c^2+2A_rA_c\cos(\phi_r-\phi_c)}, \quad (6)$$

$$\phi_{r+c}=a\tan\{[A_r\sin(\phi_r)+A_c\sin(\phi_c)]/[A_r\cos(\phi_r)+A_c\cos(\phi_c)]\}. \quad (7)$$

To test this response-based vector summation model, we used 1st harmonic amplitudes (A_r, A_c) and phases (ϕ_r, ϕ_c) of ganglion cell responses to isolated rod and cone modulation to predict responses to the combined modulation using Equation 6 and Equation 7.

The top row of Figure 6 shows the results of this analysis. The dashed lines represent perfect correspondence of predicted and measured amplitudes. The predicted amplitudes were similar to the measured amplitudes when cell responses were weak, either at low light levels (0.2 td and 2 td) or low contrast (≤0.10). At higher light levels (20 td and 200 td) and higher contrasts when cells showed larger response amplitudes (>50 impulses/s), the predicted values from the response-based vector sum model were higher than the measured values. However, the predicted phases were comparable with the measured phases for all conditions (not shown), which suggests that the deviation of predicted amplitudes from measured amplitudes might be due to response saturation (Kaplan & Shapley, 1986). Therefore, we considered a second model, which included a saturation term. As in the previous model, we assume that ganglion cell contrast responses to the combined inputs can be described by Equation 1. Starting with the recorded MC cell responses to the isolated rod and cone stimuli, we could derive an effective contrast for each response:

$$EC_r=R^{-1}(A_r), \quad (8)$$

$$EC_c=R^{-1}(A_c), \quad (9)$$

where R^{-1} is the inverse of the contrast response function. What Equation 8 or 9 does is to find the stimulus contrast, for either rod or cone modulation, that would produce a certain MC cell response amplitude. For instance, a cell gives response amplitude of 15 impulses/s to either 20% of rod modulation or 5% of combined rod–cone modulation. Then the effect contrast for 20% rod modulation (EC_r) will be 5% for combined rod–cone modulation. Similarly, we can also derive the effect contrast for cone modulation contrast (EC_c). We assumed that rod and cone inputs to MC ganglion cells could be represented as EC_r and EC_c, respectively. We further assumed that EC_r and EC_c had phases of ϕ_r and ϕ_c. A vector sum was applied to EC_r and EC_c:

$$EC_{r+c}=\sqrt{(EC_r^2+EC_c^2+2EC_rEC_c\cos(\phi_r-\phi_c)}. \quad (10)$$

The predicted amplitude were obtained as

$$A_{r+c}=R_0+\frac{R_{max}EC_{r+c}}{EC_{r+c}+C_{sat}}. \quad (11)$$

We call this model the input-based vector sum model. The recorded MC cell response amplitude versus the predicted amplitude using the input-based vector sum model versus the measured amplitude is shown in Figure 6 (bottom row). In contrast to the response-based vector sum model, the predicted values from the input-based model were closely comparable with the measured values, even for those conditions (typically with higher light and contrast levels) in which the cells had high response amplitudes. These results suggest that the MC responses to the combined stimuli could be described as a linear summation of rod and cone inputs prior to the site of saturation.

Linking human temporal contrast sensitivity functions with MC pathway temporal response

Psychophysical TCSFs with the isolated rod stimuli, isolated cone luminance stimuli, and combined rod and cone luminance stimuli at four light levels (0.2, 2, 20, 200 td) were obtained from two observers (*AB* and *YL*). Results from the two observers were quite similar and their data were averaged and are shown in Figure 7A. The TCSFs with the isolated cone stimuli at 0.2 td was not measurable. At 0.2 and 2 td, the TCSFs with the combined stimuli (triangles) were closer to those with the isolated rod stimuli (circles) than to the TCSFs with the isolated cone stimuli (squares). At higher light levels (20 and 200 td), the TCSFs with isolated cone stimuli were almost the same as those with the combined stimuli and were about 0.7 log unit higher than the TCSFs with the isolated rod stimuli.

Since MC cell responses with different stimulus types varied with eccentricity (Figure 2B) while psychophysical measurements were obtained at 6° eccentricity, we only used responses from cells with eccentricities less than 10° (N = 6, mean eccentricity of 5.6°, Figure 2B) for comparison with psychophysical TCSFs. The averaged MC cell response amplitudes at various temporal frequencies are shown in Figure 7B. As with human TCSFs, the cell responses to the isolated rod stimuli and to the combined stimuli were comparable at 0.2 and 2 td, while the responses to the isolated cone stimuli and to the combined stimuli were comparable at 20 and 200 td.

We used the contrast response function to link physiological and psychophysical measurements. By the definition of contrast gain, the linear portion of MC cell responses at low contrast could be described as

$$R=R_0+gC, \quad (12)$$

where g is the contrast gain (initial slope) and C is contrast. For a threshold response R_{th}, the contrast threshold, C_{th}, will be

$$C_{th}=(R_{th}-R_0)/g. \quad (13)$$

Then, the contrast sensitivity will be

$$Sen=1/C_{th}=g/(R_{th}-R_0). \quad (14)$$

Since we measured contrast gain only at 4.88 Hz (Figure 5), we assumed that contrast gain at other temporal frequencies was proportional to the gain at 4.88 Hz, with the proportion defined

as the ratio between response amplitudes at a specific frequency and at 4.88 Hz. With this assumption, we attempted to correlate human temporal contrast sensitivity to MC cell responses. We set the criterion response R_{th} as 8 impulses/s for all conditions to define MC cell contrast sensitivity. We then fitted 4th-order polynomials to MC cell contrast sensitivities as a function of temporal frequency for each stimulus type and light level to identify the MC cell sensitivity at the temporal frequency that was used for human TCSF measurements. Figure 8 shows the ratio of human contrast sensitivity to MC cell contrast sensitivity at each temporal frequency, stimulus type, and light level. For the majority of stimulus types and light levels, the ratios fell approximately within the range of 0.5 to 2.0, indicating reasonable correlation between psychophysical and physiological contrast sensitivities. However, for the isolated rod stimuli at 200 td and the isolated cone stimuli at 2 td, human TCSFs were low-pass while MC cell responses were band-pass, leading to a poor correlation between psychophysical and physiological measurements.

Discussion

The use of rod and cone isolating stimuli confirms that the relative strength of rod and cone inputs to MC cells varies with light level (Lee et al., 1997). When the light level approached the scotopic range (0.2 td, near cone threshold), the responses to the combined stimuli and to the isolated rod stimuli become similar; on the other hand, when the light level entered the photopic range (200 td, near rod saturation), the responses to the combined stimuli and to the isolated cone stimuli become similar. These physiological results are consistent with psychophysical findings showing that, with a successive decrease in light level in the mesopic range, the spectral efficiency function gradually shifts from $V(\lambda)$ to $V'(\lambda)$ (e.g., Benimoff, Schneider, & Hood, 1982). In parafoveal retina, the range in which rod and cone responses were equally balanced seemed to be restricted to around 20 td, although the balance of rod and cone responses might be altered by changes in cell eccentricity, stimulus wavelength, or mean chromaticity.

The estimated rod–cone time delay was on the order of 29 ms (with a range of 15–46 ms, Figure 4), with a trend toward a shorter delay at higher light levels. This is consistent with an estimate from an earlier study, which reported a delay between 20 and 40 ms in MC cells at 2 and 20 td, using a pair of heterochromatic lights modulated in various phases (Lee et al., 1997). Under conditions of comparable rod and cone light adaptation, psychophysical estimations of rod–cone delays from detection and reaction time tasks are 8–20 ms (Cao et al., 2007;Sun et al., 2001b). These values are slightly lower than the present estimates, perhaps due to the fact that in detection or reaction time tasks, only the rising portions of the impulse response functions of the rod and cone systems are used. Several other psychophysical studies reported much larger rod–cone latency differences, on the order of 75 ms (Barbur, 1982;MacLeod, 1972;van den Berg & Spekreijse, 1977), but all of these studies employed stimulus conditions including higher cone stimulus contrast and/or greater cone light adaptation. These longer delays may have derived from a delay in rod signals arising through the rod→rod bipolar→AII amacrine pathway (Sharpe, Stockman, & MacLeod, 1989). Sharpe et al. (1989) suggested that a rod signal mediated by the rod–cone gap junction pathway shows a delay of only 30 ms relative to the cone signal, consistent with our measurements.

Between 0.2 and 200 td, the measured rod and cone contrast gains in MC cells were closely similar to those derived from reaction time distribution modeling (Cao & Pokorny, 2010). It is expected that contrast gain to cone stimuli or combined stimuli will increase with light level (Purpura et al., 1988). The rod contrast gain did not vary between 2 and 200 td, although there was a phase advance with increased light level (Figure 3). The light levels used in the current study were in the linear portion of the Aguilar–Stiles scotopic TVI function (−2 to 2 log scotopic td, Aguilar & Stiles, 1954). A linear relationship in the TVI function indicates that a constant

contrast is required for detection. This translates into a constant contrast gain assuming a linear relationship between psychophysical contrast sensitivity and cell response amplitude. Importantly, while the shapes of the temporal modulation transfer functions with the isolated cone stimuli change dramatically as light levels increase (particularly from 20 td to 200 td, see Figure 1A), the shapes of the temporal modulation transfer functions with the isolated rod stimuli do not vary much (the frequency with peak response amplitude was between 2 and 10 Hz). This implies that the mechanisms that modify temporal response in MC cells with light level to achieve Weber's law (Dunn, Lankheet, & Rieke, 2007; Smith, Pokorny, Lee, & Dacey, 2008) are limited to cones; rod responses show Weber behavior (Figure 5) but do not show major changes in their temporal responses with light level (Figure 1).

Comparison between model predictions and cell responses (Figure 6) indicated that the input-based vector sum model predicts the response amplitudes better than the response-based vector sum model. The results are consistent with earlier findings from cat ganglion cells (Enroth-Cugell, Hertz, & Lennie, 1977). Brief pulses (50 ms) stimulating rods alone, cones alone, or rods and cones simultaneously were applied on mesopic backgrounds. When pulses were weak, simple linear addition of rod and cone responses predicted the responses to combined stimuli; when pulses were strong, the simple sum of rod and cone responses was larger than the combined responses. With our sinusoidal stimuli, the difference in rod and cone response phase required a vector sum, instead of a simple linear sum, to describe the combination of rod and cone responses. Our analysis further indicated that a response-based vector sum of rod and cone responses fails to describe the response to the combined stimuli due to response saturation.

The improvement in fit with the input-based vector sum model suggests linear combination of rod and cone signals before the site of saturation. Response saturation in MC cells is usually associated with a phase advance with increasing contrast (Benardete, Kaplan, & Knight, 1992; Yeh, Lee, & Kremers, 1995) and thought to be due to contrast gain controls (Lee, Pokorny, Smith, & Kremers, 1994; Shapley & Victor, 1979b). We looked for a phase advance associated with rod responses, but the data were noisy. The locus of contrast gain control is uncertain but appears to be after spatial summation has occurred (Shapley & Victor, 1979a). A phase advance of spike activity relative to the membrane potential modulation has been seen in cat ganglion cells with increasing contrast (Lankheet, Molenaar, & van de Grind, 1989). In any event, our data suggest that response saturation occurs after combination of rod and cone signals.

Psychophysically, it was shown that a linear vector sum model could account for the temporal combination of rod and cone signals that mediated flicker detection (Kremers & Meierkord, 1999; MacLeod, 1972; van den Berg & Spekreijse, 1977). Others, however, showed an incomplete addition in increment detection (Buck & Knight, 1994; Drum, 1982). Psychophysical measurements of mesopic luminance could be modeled as a log sum of $V(\lambda)$ to $V'(\lambda)$ (Ikeda & Shimozono, 1981; Yaguchi & Ikeda, 1984). Our MC cell recordings may reconcile these different findings in psychophysics: incomplete summation of rod and cone signals might be due to saturation of responses in the MC pathway, especially for suprathreshold tasks (Benimoff et al., 1982; Kremers & Meierkord, 1999).

The psychophysical TCSFs were consistent with MC cell responses except at high frequencies. It has been shown (Lee, Sun, & Zucchini, 2007) that MC cell response variability increases dramatically with temporal frequency, which could largely account for the difference in shapes between psychophysical TCSFs and physiological TCSFs (based on peak MC cell firing rate) at photopic levels. Estimates of response variability in our experiments suggested a similar conclusion. At low frequency (1 Hz), the measured TCSF was slightly higher than MC cell responses. It might be caused by the edge effect in our psychophysical measurement of TCSFs (Kelly, 1959; Spehar & Zaidi, 1997).

Which rod pathway mediates rod signals at mesopic light levels? It has been proposed that only the rod–cone gap junction pathway is active at mesopic levels (Daw et al., 1990; Sharpe & Stockman, 1999). However, physiological recordings indicate that AII amacrine cells respond at light levels within the mesopic range (Dacey, 1999; Manookin, Beaudoin, Ernst, Flagel, & Demb, 2008; Pang, Gao, & Wu, 2002; Xin & Bloomfield, 1999) and it has also been suggested that the rod→rod bipolar→AII amacrine pathway mediates strong inputs in MC cells at 2–20 td (Lee et al., 1997). In the current MC cell measurements, the rod/cone response ratios at 20 or 200 td were relatively stable at frequencies ≤10 Hz. At 2 td, however, the rod/cone response ratios decreased with temporal frequency. Further, the shape of temporal response function with the isolated rod stimuli is relatively stable at lower light levels (0.2–20 td). These results might suggest that the rod→rod bipolar→AII amacrine pathway mediates visual functions at low mesopic light levels and the rod–cone gap junction at higher light levels. Our preliminary measurements indicated that MC cell receptive fields defined by rod and cone inputs at mesopic light levels differ (Cao, Lee, & Ennis, 2010), which also suggests the involvement of the rod→rod bipolar→AII amacrine pathway, because it is expected that receptive fields defined by rod and cone inputs should be similar under conditions where the rod– cone gap junction pathway mediates mesopic vision (Verweij, Peterson, Dacey, & Buck, 1999). It has also been proposed that signals from the two rod pathways can cancel one another. With a 15-Hz modulation in a range of 0.07–0.2 td (using a long-wavelength adapting light to selectively desensitize cones, although rod isolation may not be complete with this strategy), both psychophysical (Conner, 1982; Sharpe et al., 1989) or electrophysiological (Stockman, Sharpe, Ruther, & Nordby, 1995) results were consistent with such cancellation. If so, we would expect with the isolated rod stimuli at 13 Hz and 0.2 td that the response amplitude would be reduced sharply due to cancellation (Stockman et al., 1995). However, we did not observe this phenomenon in MC cell responses (Figure 1A, top panel), suggesting that cancellation of rod signals from the two-rod pathways may have other etiologies. Taken together, our study suggests that the rod–cone gap junction alone does not mediate mesopic vision, and we do not have evidence for simultaneous activation of the two-rod pathways. It is possible that the rod→rod bipolar→AII amacrine pathway dominates at low mesopic light level while the rod–cone gap junction pathway dominates at higher mesopic light levels, but this remains an open question.

Acknowledgments

This study was supported by National Eye Institute Grants R01EY019651 (D. Cao) and R01EY013112 (B. B. Lee). We thank Joel Pokorny for his comments on this manuscript.

References

Aguilar M, Stiles WS. Saturation of the rod mechanism of the retina at high levels of illumination. Optica Acta 1954;1:59–65.

Barbur JL. Reaction-time determination of the latency between visual signals generated by rods and cones. Ophthalmic & Physiological Optics 1982;2:179–185. [PubMed: 7177643]

Benardete EA, Kaplan E, Knight BW. Contrast gain control in the primate retina: P cells are not X-like, some M cells are. Visual Neuroscience 1992;8:483–486. [PubMed: 1586649]

Benimoff N, Schneider S, Hood DC. Interactions between rod and cone channels above threshold: A test of various models. Vision Research 1982;22:1133–1140. [PubMed: 7147724]

Buck, SL. Rod–cone interaction in human vision. In: Chalupa, LM.; Werner, JS., editors. The visual neuroscience. Vol. vol. 1. Cambridge, MA: MIT Press; 2004. p. 863-878.

Buck SL, Knight R. Partial additivity of rod signals with M- and L-cone signals in increment detection. Vision Research 1994;34:2537–2545. [PubMed: 7975293]

Buck SL, Knight RF, Bechtold J. Opponent-color models and the influence of rod signals on the loci of unique hues. Vision Research 2000;40:3333–3344. [PubMed: 11058732]

Cao D, Lee BB, Ennis R. Receptive field structure of primate parasol ganglion cells defined by rod and cone inputs. Investigative Opthalmology & Visual Science. 2010 ARVO-E Abstract 5177.

Cao D, Pokorny J. Rod and cone contrast gains derived from reaction time distribution modeling. Journal of Vision 2010;10(2):11, 1–15. http://www.journalofvision.org/content/10/2/11, doi:10.1167/10.2.11. [PubMed: 20462312]

Cao D, Pokorny J, Smith VC. Matching rod percepts with cone stimuli. Vision Research 2005;45:2119–2128. [PubMed: 15845243]

Cao D, Pokorny J, Smith VC, Zele AJ. Rod contributions to color perception: Linear with rod contrast. Vision Research 2008;48:2586–2592. [PubMed: 18561973]

Cao D, Zele AJ, Pokorny J. Dark-adapted rod suppression of cone flicker detection: Evaluation of receptoral and postreceptoral interactions. Visual Neuroscience 2006;23:531–537. [PubMed: 16961991]

Cao D, Zele AJ, Pokorny J. Linking impulse response functions to reaction time: Rod and cone reaction time data and a computational model. Vision Research 2007;47:1060–1074. [PubMed: 17346763]

Cao D, Zele AJ, Pokorny J. Chromatic discrimination in the presence of incremental and decremental rod pedestals. Visual Neuroscience 2008;25:399–404. [PubMed: 18598409]

Conner JD. The temporal properties of rod vision. The Journal of Physiology 1982;332:139–155. [PubMed: 7153925]

Crook JD, Davenport CM, Peterson BB, Packer O, Detwiler PB, Dacey DM. Parallel ON and OFF cone bipolar inputs establish spatially coextensive receptive field structure of blue-yellow ganglion cells in primate retina. Journal of Neuroscience 2009;29:8372–8387. [PubMed: 19571128]

Crook JM, Lange-Malecki B, Lee BB, Valberg A. Visual resolution of macaque retinal ganglion cells. The Journal of Physiology 1988;396:205–224. [PubMed: 3411497]

Curcio CA, Sloan KR, Kalina RE, Hendrickson AE. Human photoreceptor topography. Journal of Comparative Neurology 1990;292:497–523. [PubMed: 2324310]

Dacey DM. Primate retina: Cell types, circuits and color opponency. Progress in Retinal and Eye Research 1999;18:737–763. [PubMed: 10530750]

Dacey DM. Parallel pathways for spectral coding in primate retina. Annual Review of Neuroscience 2000;23:743–775.

Daw NW, Jensen EJ, Brunken WJ. Rod pathways in the mammalian retinae. Trends in Neurosciences 1990;13:110–115. [PubMed: 1691871]

Drum B. Summation of rod and cone responses at absolute threshold. Vision Research 1982;22:823–826. [PubMed: 7123867]

Dunn FA, Lankheet MJ, Rieke F. Light adaptation in cone vision involves switching between receptor and post-receptor sites. Nature 2007;449:603–607. [PubMed: 17851533]

Enroth-Cugell C, Hertz BG, Lennie P. Convergence of rod and cone signals in the cat's retina. The Journal of Physiology 1977;269:297–318. [PubMed: 894595]

Estévez O, Spekreijse H. The "silent substitution" method in visual research. Vision Research 1982;22:681–691. [PubMed: 7112962]

Field GD, Greschner M, Gauthier JL, Rangel C, Shlens J, Sher A, et al. High-sensitivity rod photoreceptor input to the blue-yellow color opponent pathway in macaque retina. Nature Neuroscience 2009;12:1159–1164.

Gouras P, Link K. Rod and cone interaction in dark-adapted monkey ganglion cells. The Journal of Physiology 1966;184:499–510. [PubMed: 4958644]

Ikeda M, Shimozono H. Mesopic luminous-efficiency functions. Journal of the Optical Society of America 1981;71:280–284. [PubMed: 7218072]

Kaplan E, Shapley RM. The primate retina contains two types of ganglion cells, with high and low contrast sensitivity. Proceedings of the National Academy of Sciences of the United States of America 1986;83:2755–2757. [PubMed: 3458235]

Kelly DH. Effects of sharp edges in a flickering field. Journal of the Optical Society of America 1959;49:730–732. [PubMed: 13655165]

Kremers J, Meierkord S. Rod-cone interactions in deuteranopic observers: Models and dynamics. Vision Research 1999;39:3372–3385. [PubMed: 10615502]

Kremers J, Scholl HPN. Rod-/L-cone and rod-/M-cone interactions in electroretinograms at different temporal frequencies. Visual Neuroscience 2001;18:339–351. [PubMed: 11497411]

Lankheet MJM, Molenaar J, van de Grind WA. The spike generating mechanism of cat retinal ganglion cells. Vision Research 1989;29:505–517. [PubMed: 2603388]

Lee BB, Martin PR, Valberg A. Sensitivity of macaque retinal ganglion cells to chromatic and luminance flicker. The Journal of Physiology 1989;414:223–243. [PubMed: 2607430]

Lee BB, Pokorny J, Smith VC, Kremers J. Responses to pulses and sinusoids in macaque ganglion cells. Vision Research 1994;34:3081–3096. [PubMed: 7975341]

Lee BB, Pokorny J, Smith VC, Martin PR, Valberg A. Luminance and chromatic modulation sensitivity of macaque ganglion cells and human observers. Journal of the Optical Society of America A 1990;7:2223–2236.

Lee BB, Smith VC, Pokorny J, Kremers J. Rod inputs to macaque ganglion cells. Vision Research 1997;37:2813–2828. [PubMed: 9415362]

Lee BB, Sun H, Zucchini W. The temporal properties of the response of macaque ganglion cells and central mechanisms of flicker detection. Journal of Vision 2007;7(1):1, 1–16. http://www.journalofvision.org/content/7/14/1, doi: 10.1167/7.14.1.

MacLeod DI. Rods cancel cones in flicker. Nature 1972;235:173–174. [PubMed: 4551230]

Manookin MB, Beaudoin DL, Ernst ZR, Flagel LJ, Demb JB. Disinhibition combines with excitation to extend the operating range of the OFF visual pathway in daylight. Journal of Neuroscience 2008;28:4136–4150. [PubMed: 18417693]

Pang JJ, Gao F, Wu SM. Relative contributions of bipolar cell and amacrine cell inputs to light responses of ON, OFF and ON-OFF retinal ganglion cells. Vision Research 2002;42:19–27. [PubMed: 11804628]

Pokorny, J.; Cao, D. CIE Symposium “Lighting Quality & Energy Efficiency”. Vol. x035. Vienna, Austria: CIE; 2010. Rod and cone contributions to mesopic vision. In Commission Internationale de l’Eclairage (Ed.); p. 9-20.

Pokorny, J.; Smith, VC. Chromatic discrimination. In: Chalupa, LM.; Werner, JS., editors. The visual neuroscience. Vol. vol. 2. Cambridge, MA: MIT Press; 2004. p. 908-923.

Pokorny J, Smithson H, Quinlan J. Photo-stimulator allowing independent control of rods and the three cone types. Visual Neuroscience 2004;21:263–267. [PubMed: 15518198]

Purpura K, Kaplan E, Shapley RM. Background light and the contrast gain of primate P and M retinal ganglion cells. Proceedings of the National Academy of Sciences of the United States of America 1988;85:4534–4537. [PubMed: 3380804]

Puts MJH, Pokorny J, Quinlan J, Glennie L. Audiophile hardware in vision science; the soundcard as a digital to analog converter. Journal of Neuroscience Methods 2005;142:77–81. [PubMed: 15652619]

Shapiro AG, Pokorny J, Smith VC. Cone- rod receptor spaces, with illustrations that use CRT phosphor and light-emitting-diode spectra. Journal of the Optical Society of America A 1996;13:2319–2328.

Shapley RM, Enroth-Cugell C. Visual adaptation and retinal gain controls. Progress in Retinal and Eye Research 1984;3:263–346.

Shapley RM, Victor JD. Nonlinear spatial summation and the contrast gain control of cat retinal ganglion cells. The Journal of Physiology 1979a;290:141–161. [PubMed: 469742]

Shapley RM, Victor JD. The contrast gain control of the cat retina. Vision Research 1979b;19:431–434. [PubMed: 473613]

Sharpe LT, Stockman A. Rod pathways: The importance of seeing nothing. Trends in Neurosciences 1999;22:497–504. [PubMed: 10529817]

Sharpe LT, Stockman A, MacLeod DI. Rod flicker perception: Scotopic duality, phase lags and destructive interference. Vision Research 1989;29:1539–1559. [PubMed: 2635479]

Smith VC, Lee BB, Pokorny J, Martin PR, Valberg A. Responses of macaque ganglion cells to the relative phase of heterochromatically modulated lights. The Journal of Physiology 1992;458:191–221. [PubMed: 1302264]

Smith VC, Pokorny J. The design and use of a cone chromaticity space. Color Research and Application 1996;21:375–383.

Smith VC, Pokorny J, Lee BB, Dacey DM. Sequential processing in vision: The interaction of sensitivity regulation and temporal dynamics. Vision Research 2008;48:2649–2656. [PubMed: 18558416]

Spehar B, Zaidi Q. Surround effects on the shape of the temporal contrast-sensitivity function. Journal of the Optical Society of America A 1997;14:2517–2525.

Stabell U, Stabell B. Wavelength discrimination of peripheral cones and its change with rod intrusion. Vision Research 1977;17:423–426. [PubMed: 878331]

Stockman A, Sharpe LT, Ruther K, Nordby K. Two signals in the human rod visual system: A model based on electrophysiological data. Visual Neuroscience 1995;12:951–970. [PubMed: 8924418]

Sun H, Pokorny J, Smith VC. Brightness Induction from rods. Journal of Vision 2001a;1(1):4, 32–41. http://www.journalofvision.org/content/1/1/4, doi:10.1167/1.1.4.

Sun H, Pokorny J, Smith VC. Rod–cone interactions assessed in inferred postreceptoral pathways. Journal of Vision 2001b;1(1):5, 42–54. http://www.journalofvision.org/content/1/1/5, doi:10.1167/1.1.5.

Swanson WH, Ueno T, Smith VC, Pokorny J. Temporal modulation sensitivity and pulse detection thresholds for chromatic and luminance perturbations. Journal of the Optical Society of America A 1987;4:1992–2005.

van den Berg TJTP, Spekreijse H. Interaction between rod and cone signals studied with temporal sine wave stimulation. Journal of the Optical Society of America 1977;67:1210–1217. [PubMed: 903846]

Verweij J, Peterson BB, Dacey DM, Buck SL. Sensitivity and dynamics of rod signals in H1 horizontal cells of the macaque monkey retina. Vision Research 1999;39:3662–3672. [PubMed: 10746136]

Virsu V, Lee BB. Light adaptation in cells of macaque lateral geniculate nucleus and its relation to human light adaptation. Journal of Neurophysiology 1983;50:864–878. [PubMed: 6631467]

Virsu V, Lee BB, Creutzfeldt OD. Mesopic spectral responses and the Purkinje shift of macaque lateral geniculate cells. Vision Research 1987;27:191–200. [PubMed: 3576979]

Wiesel T, Hubel DH. Spatial and chromatic interactions in the lateral geniculate body of the rhesus monkey. Journal of Neurophysiology 1966;29:1115–1156. [PubMed: 4961644]

Xin D, Bloomfield SA. Comparison of the responses of AII amacrine cells in the dark- and light-adapted rabbit retina. Visual Neuroscience 1999;16:653–665. [PubMed: 10431914]

Yaguchi H, Ikeda M. Mesopic luminous-efficiency functions for various adapting levels. Journal of the Optical Society of America A 1984;1:120–123.

Yeh T, Lee BB, Kremers J. The temporal response of ganglion cells of the macaque retina to cone-specific modulation. Journal of the Optical Society of America A 1995;12:456–464.

Zele AJ, Cao D, Pokorny J. Threshold units: A correct metric for reaction time? Vision Research 2007;47:608–611. [PubMed: 17240416]

Zele AJ, Cao D, Pokorny J. Rod-cone interactions and the cone pathway temporal impulse response. Vision Research 2008;48:2593–2598. [PubMed: 18486960]

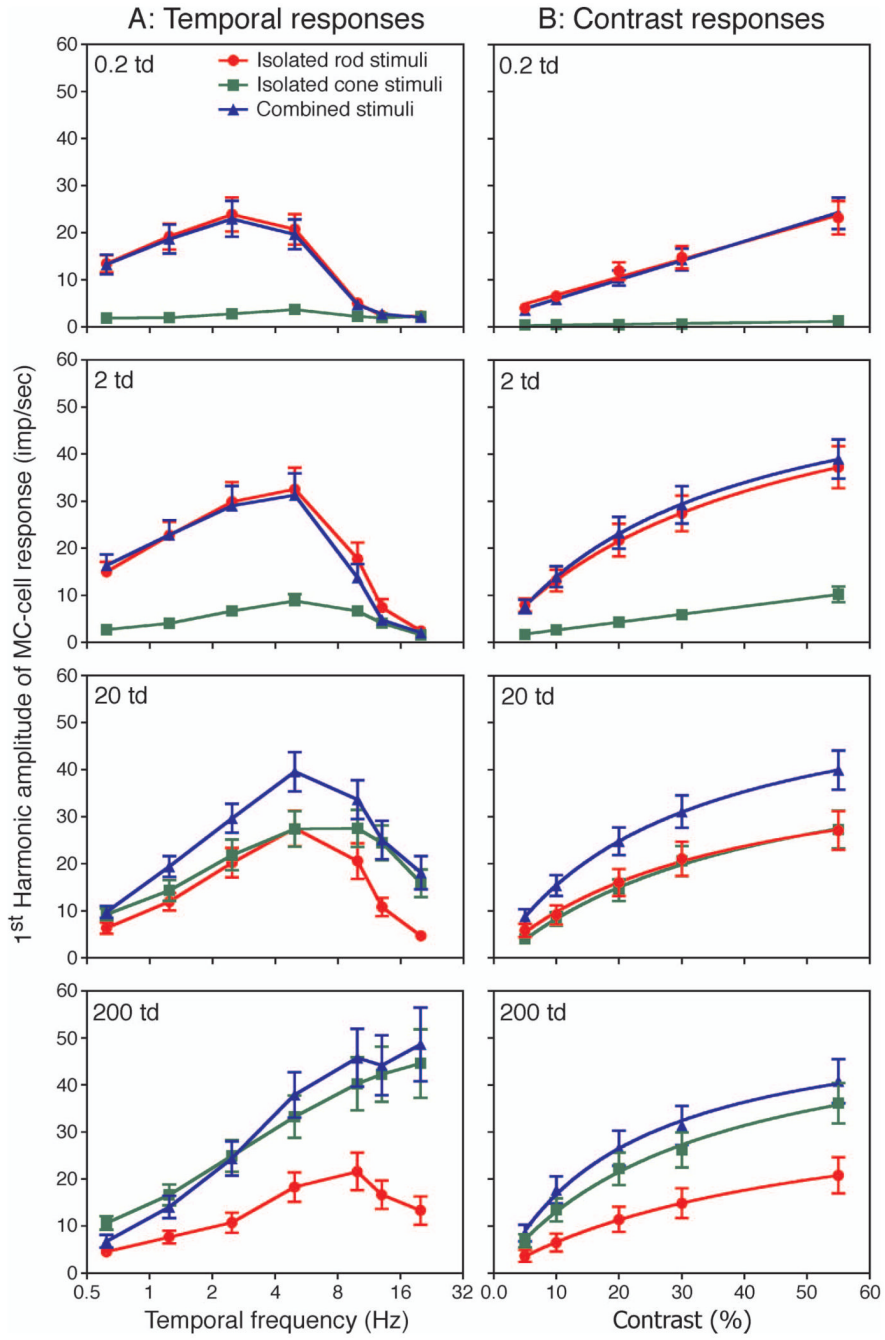

Figure 1.

The averaged 1st harmonic amplitudes (impulse per second, first harmonics) of MC cell responses with the isolated rod stimuli (circles), isolated cone stimuli (squares), and combined rod and cone stimuli (triangles) at 0.2, 2, 20, and 200 td. (A) Temporal frequency response function measured at 55% contrast. (B) Contrast response function measured at 4.88 Hz (the lines are fits of the Michaelis–Menten equation). Error bars are standard errors.

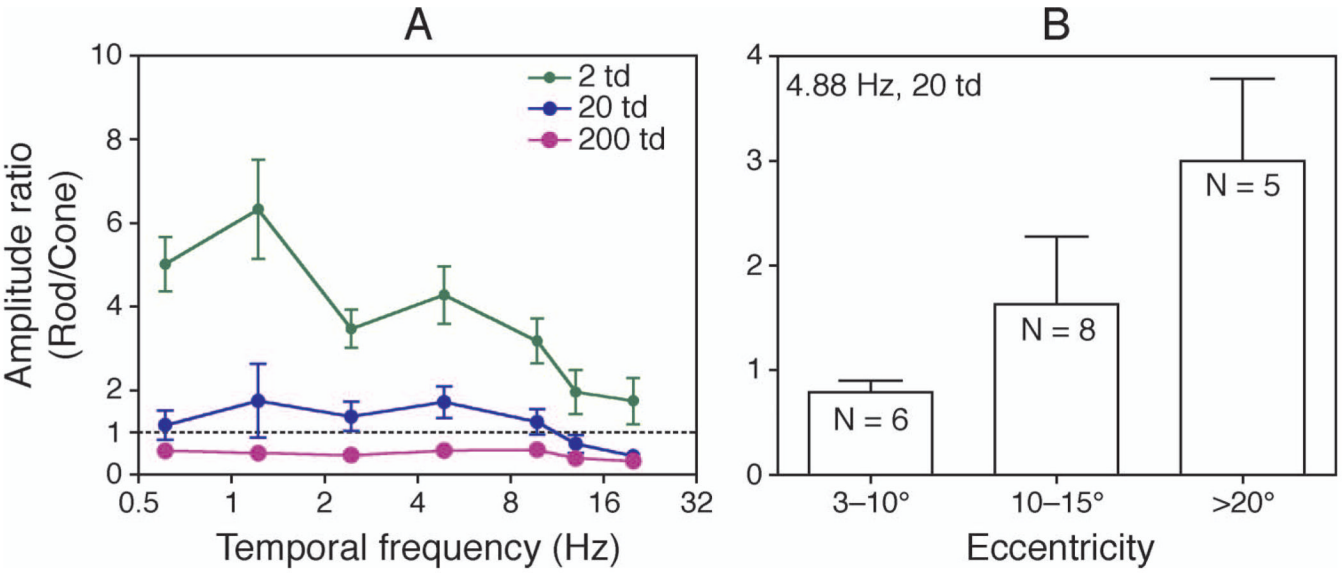

Figure 2.

The ratios of response amplitudes to the isolated rod and cone stimuli. (A) The rod/cone ratios at different temporal frequencies and light levels averaged from all cells (therefore all eccentricities) are plotted, the dashed lines representing equal rod and cone response amplitudes. (B) The rod/cone ratios measured at 4.88 Hz and 20 td with different retinal eccentricity. The rod/cone ratios increased with increasing eccentricity (analysis of variance, $p = 0.002$). Error bars are standard errors.

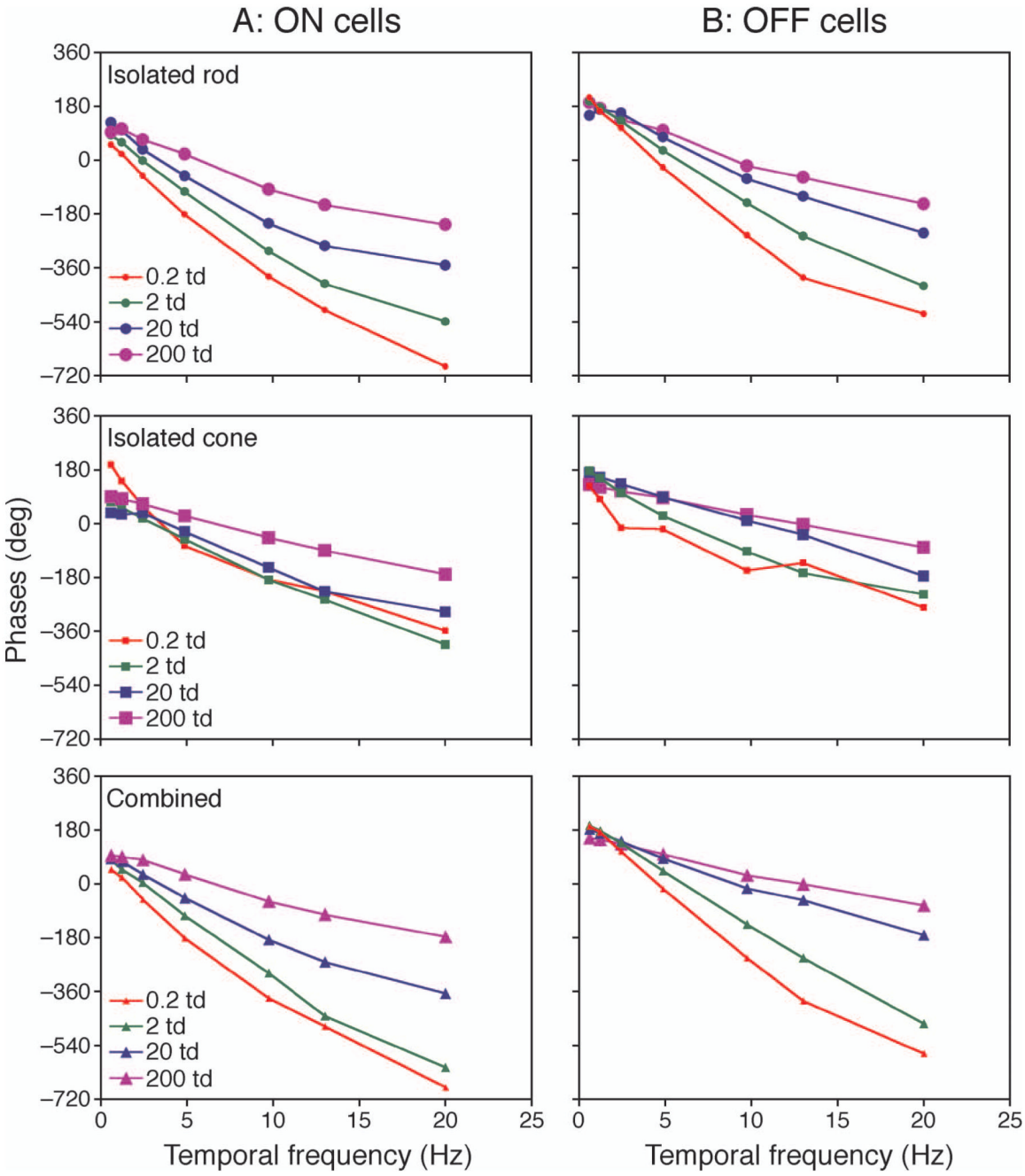

Figure 3.

The averaged phases from the cells that showed strong responses to both the isolated rod and cone stimuli (peak amplitude ≥10 impulses/s). (A) On cells (1 cell at 0.2 td, 6 cells at 2 td, 7 cells at 20 td, and 7 cells at 200 td). (B) Off cells (3 cells at 0.2 td, 9 cells at 2 td, 8 cells at 20 td, and 9 cells at 200 td). Error bars are standard errors.

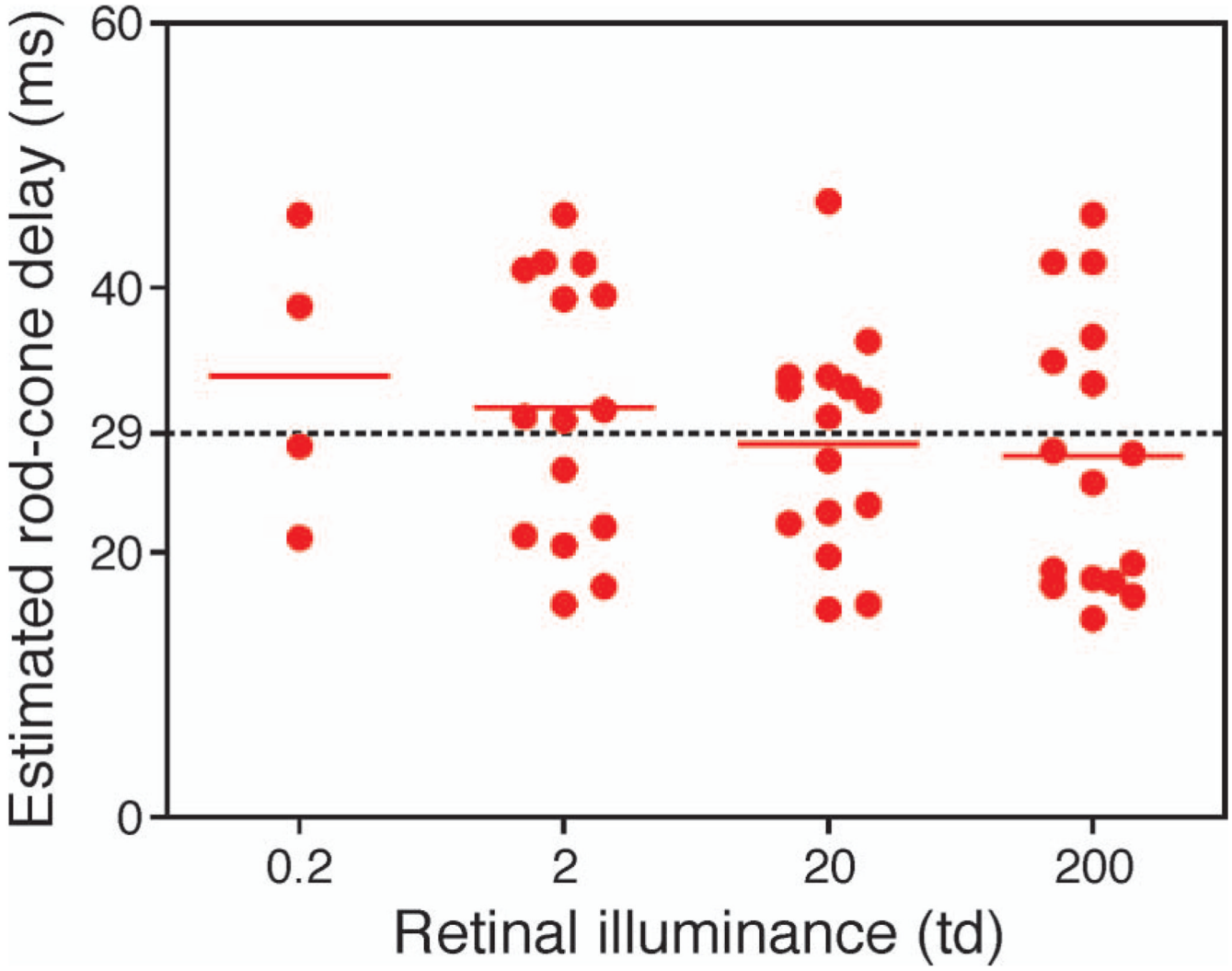

Figure 4.
The estimated rod–cone delays at 0.2, 2, 20, and 200 td. There was a trend that rod–cone delays decreased with increased light levels. The dash line is the grand mean delay at all light levels (29 ms).

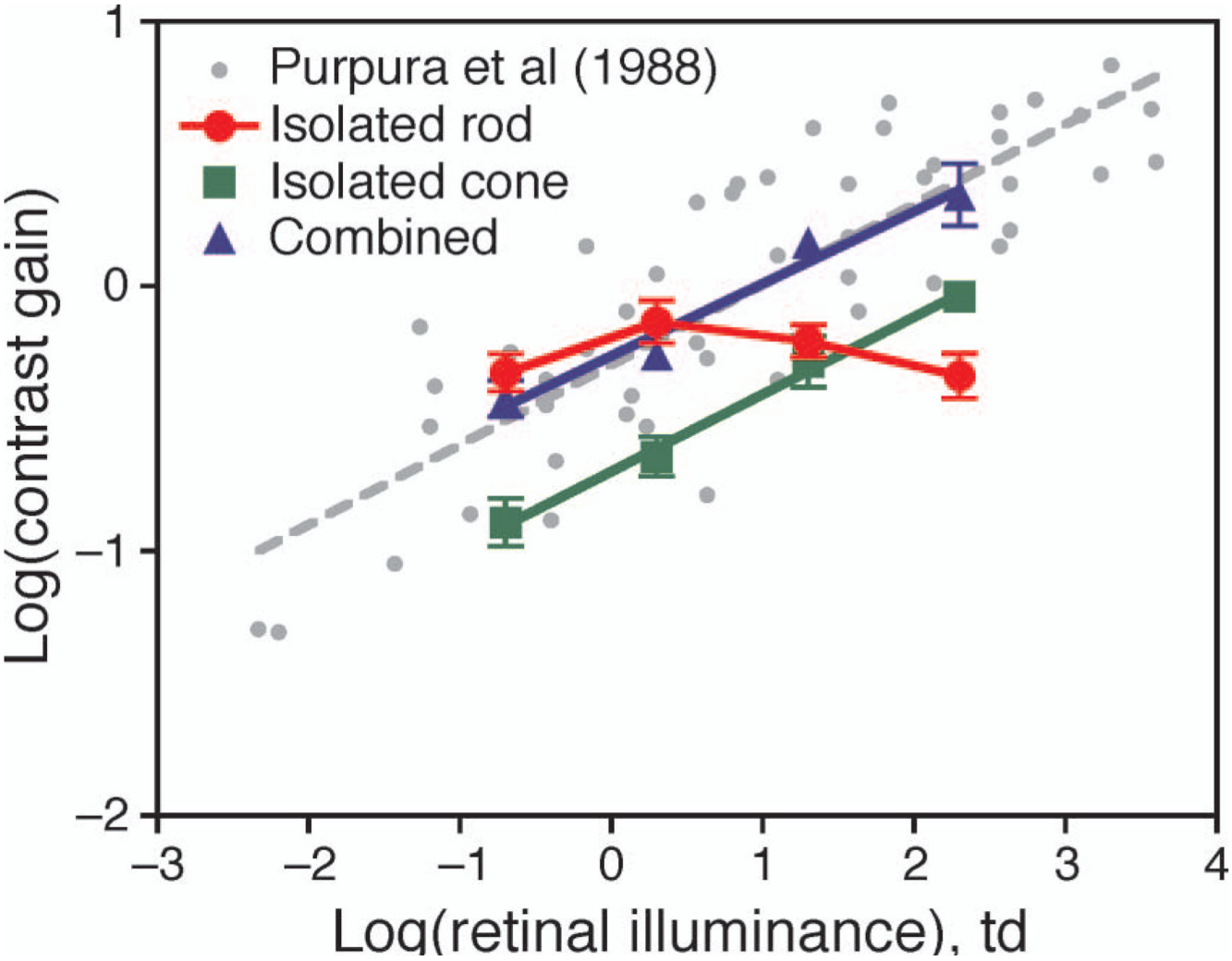

Figure 5.
Contrast gains with different stimulus types in the context of the measured contrast gain by Purpura et al. (1988), in a log–log plot. The gray dashed line is the linear fit of Purpura et al.'s data. The solid lines are linear fits of the estimated contrast gains for the isolated cone or combined stimuli. Error bars are standard errors.

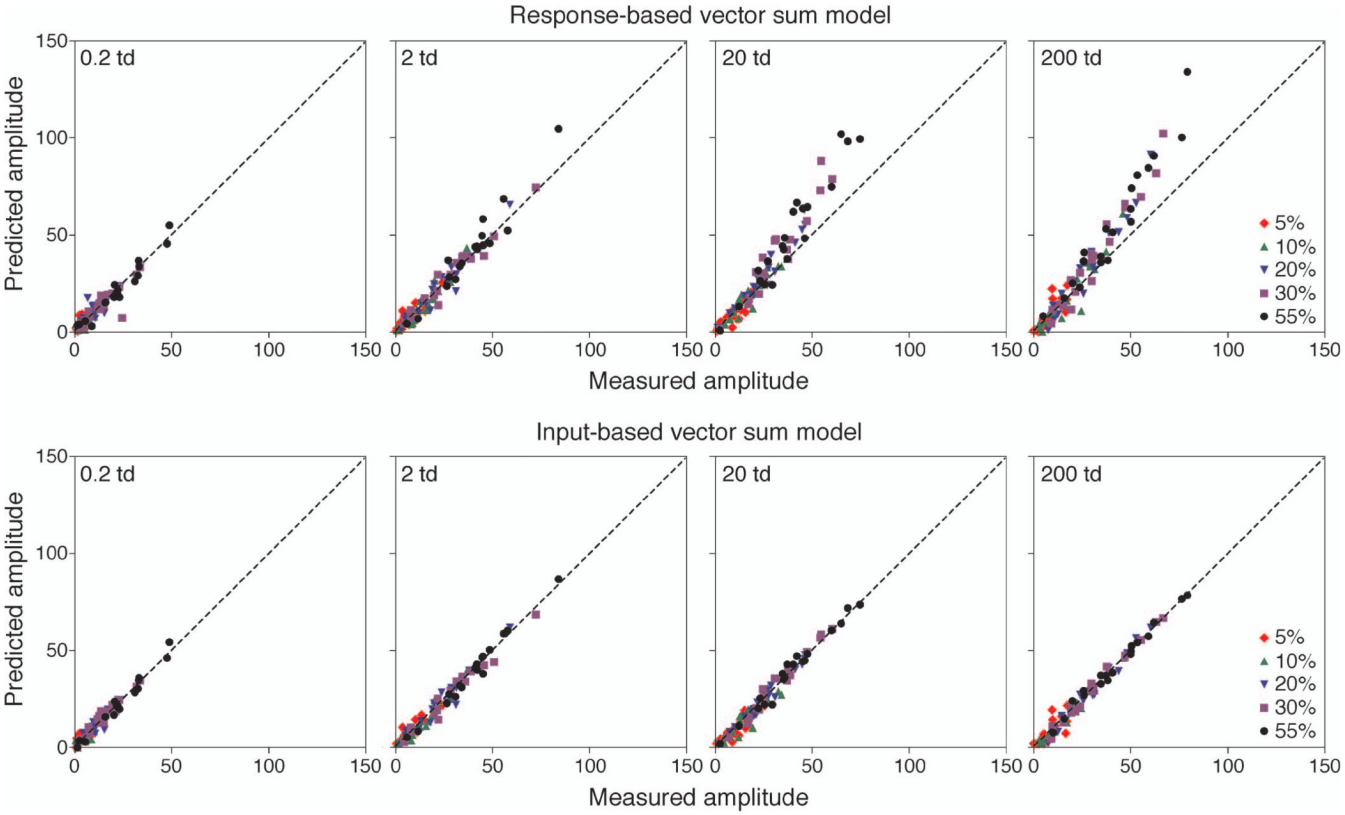

Figure 6.

The comparison between the predicted amplitudes and the measured amplitudes to the combined stimuli from (top) the response-based vector sum model and (bottom) the input-based vector sum model. The dashed lines represent perfect correspondence between the predicted and measured amplitudes.

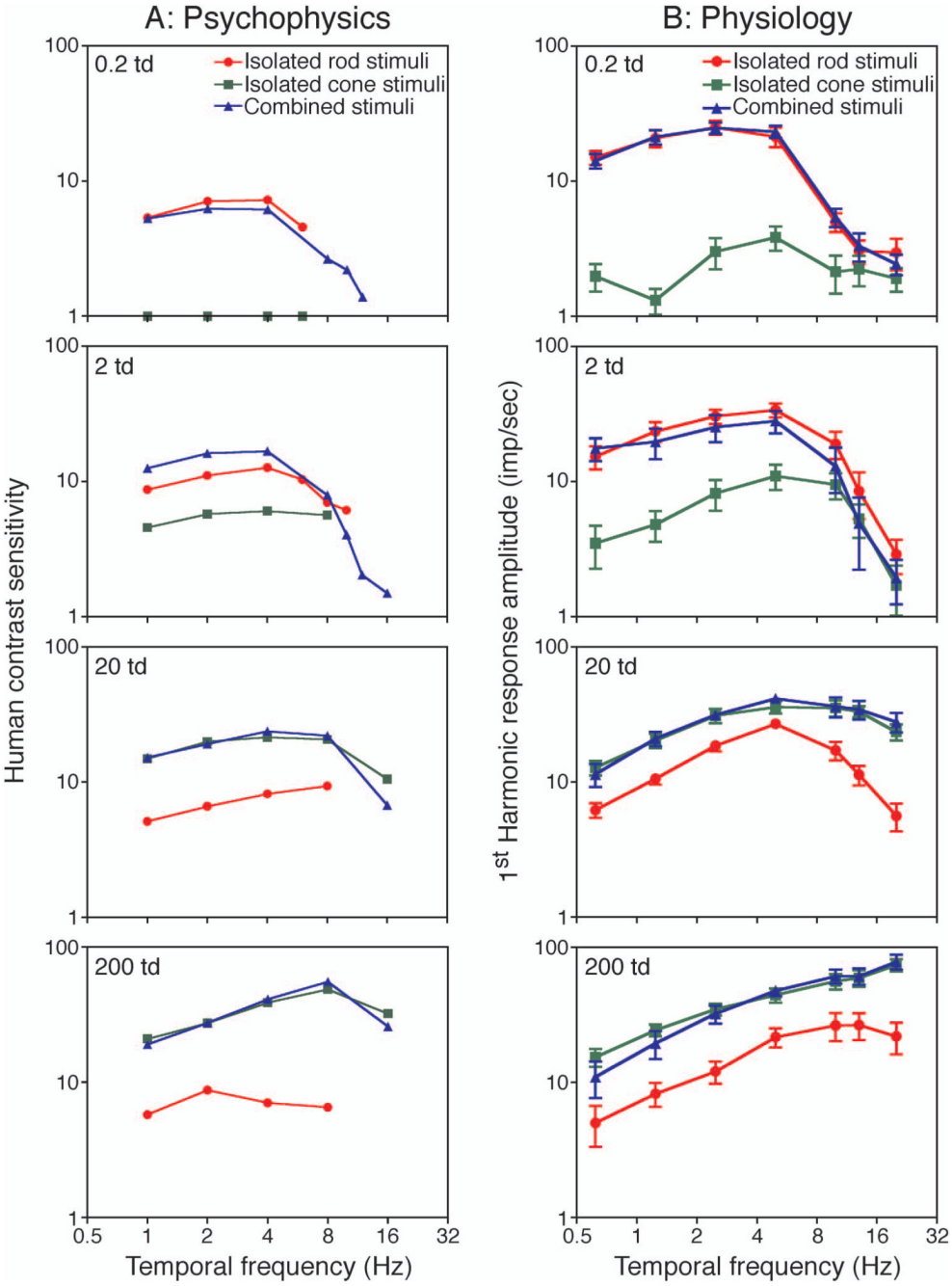

Figure 7.

Human temporal contrast sensitivity function (TCSF) and MC cell response amplitudes with eccentricities ≤10°. (A) Averaged TCSFs from two observers to the isolated rod stimuli (circles), isolated cone stimuli (squares), and combined rod and cone stimuli (triangles). (B) The averaged MC cell response amplitudes (eccentricities between 3° and 10°, $N = 6$ cells).

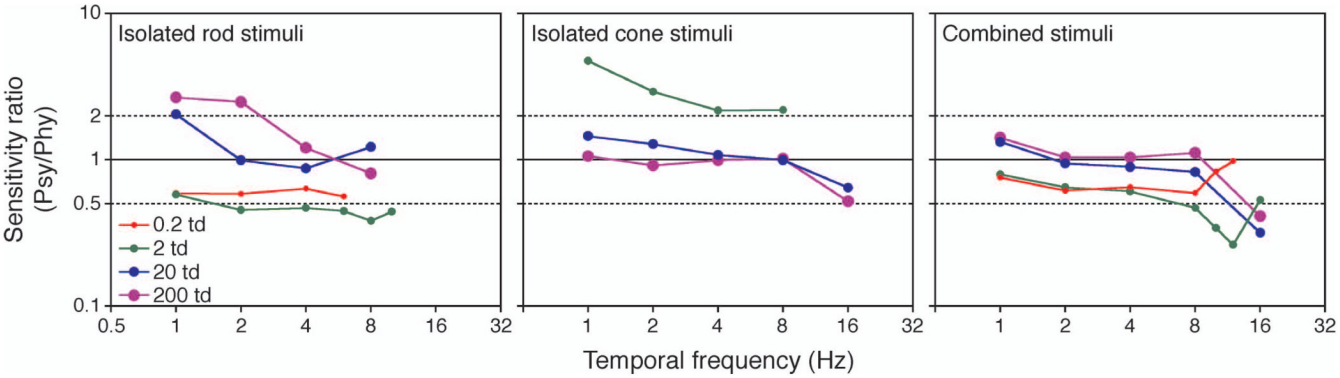

Figure 8.
The ratios of human contrast sensitivities to MC cell contrast sensitivities with (left) the isolated rod stimuli, (middle) the isolated cone stimuli, and (right) the combined stimuli.